NERC Open Research Archive
sharing our research

Centre for Ecology & Hydrology
NATURAL ENVIRONMENT RESEARCH COUNCIL

Article (refereed) - postprint

Hou, Xikang; Zhan, Xiaoying; Zhou, Feng; Yan, Xiaoyuan; Gu, Baojing; Reis, Stefan; Wu, Yali; Liu, Hongbin; Piao, Shilong; Tang, Yanhong. 2018.
Detection and attribution of nitrogen runoff trend in China's croplands.
Environmental Pollution, 234. 270-278.
https://doi.org/10.1016/j.envpol.2017.11.052

Detection and attribution of nitrogen runoff trend in China's croplands

Xikang Hou [1,+], Xiaoying Zhan [1,+], Feng Zhou [1,*], Xiaoyuan Yan [2], Baojing Gu [3], Stefan Reis [4,6], Yali Wu [1], Hongbin Liu [5], Shilong Piao [1], Yanhong Tang [1]

1. Sino-France Institute of Earth Systems Science, Laboratory for Earth Surface Processes, College of Urban and Environmental Sciences, Peking University, Beijing, 100871, P.R. China
2. State Key Laboratory of Soil and Sustainable Agriculture, Institute of Soil Science, Chinese Academy of Sciences, Nanjing, 210008, P.R. China
3. Department of Land Management, Zhejiang University, Hangzhou 310058, P.R. China
4. Natural Environment Research Council, Centre for Ecology & Hydrology, Bush Estate, Penicuik EH26 0QB, United Kingdom
5. Institute of Agricultural Resources and Regional Planning, Chinese Academy of Agricultural Sciences, Beijing 100081, P.R. China
6. University of Exeter Medical School, Knowledge Spa, Truro, TR1 3HD, United Kingdom

[+] X.K.H and X.Y.Z contributed equally to this work.

[*] Corresponding author. Phone: +86 10 62756511. Email: zhouf@pku.edu.cn (F. Z.)

Acronyms and Abbreviations

R_{TN}	Cropland N runoff	RR	R_{TN} per unit N fertilizer additions
R^0	Background N runoff	pH	Soil pH value
SOM	Soil organic matter	$Clay$	Soil clay content
TN	Soil total nitrogen	$Temp$	Mean air temperature
N_{rate}	Nitrogen (N) fertilizer application rate per unit sowing area	W	Sum of precipitation and irrigation within observation period
x_k	Environmental variables	CE	Correction coefficient

Abstract

Reliable detection and attribution of changes in nitrogen (N) runoff from croplands are essential for designing efficient, sustainable N management strategies for future. Despite the recognition that excess N runoff poses a risk of aquatic eutrophication, large-scale, spatially detailed N runoff trends and their drivers remain poorly understood in China. Based on data comprising 535 site-years from 100 sites across China's croplands, we developed a data-driven upscaling model and a new simplified attribution approach to detect and attribute N runoff trends during the period of 1990-2012. Our results show that N runoff has increased by 46% for rice paddy fields and 31% for upland areas since 1990. However, we acknowledge that the upscaling model is subject to large uncertainties (20% and 40% as coefficient of variation of N runoff, respectively). At national scale, increased fertilizer application was identified as the most likely driver of the N runoff trend, while decreased irrigation levels offset to some extent the impact of fertilization increases. In southern China, the increasing trend of upland N runoff can be attributed to the growth in N runoff rates. Our results suggested that increased SOM led to the N runoff rate growth for uplands, but led to a decline for rice paddy fields. In combination, these results imply that improving management approaches for both N fertilizer use and irrigation is urgently required for mitigating agricultural N runoff in China.

Keywords: Nitrogen runoff; temporal trend; spatial pattern; attribution analysis; Bayesian inference

Capsule

Cropland N runoff in China increased by 30% over the past two decades mainly due to increased fertilization and decreased irrigation.

Highlights

- A data-driven upscaling model can effectively and reliably detect N runoff trends
- N runoff has increased by 46% for rice paddy fields and 31% for uplands since 1990
- SOM change results in inverse trend of N runoff rates between upland and rice fields

1. Introduction

Meeting food security targets while simultaneously reducing reactive nitrogen losses has drawn attention from both scientists and the public (Chen et al., 2014; Mueller et al., 2012; Tilman et al., 2011; Zhang et al., 2015). Large amounts of anthropogenic nitrogen (N) inputs have resulted in excess N being lost in runoff from croplands to water bodies and the atmosphere worldwide (Cui et al., 2014; Leip et al., 2011; Seitzinger et al., 2010). As one of the consequences, increased occurrences of aquatic eutrophication and ecosystem degradation were observed, particularly in China and South Asia (Paerl et al., 2014). Reliable detection and attribution of cropland N runoff are crucial for policy makers and farmers to develop site-specific N management strategies (Cherry et al., 2008). Although cropland N runoff is substantial in China (e.g., 2.1±0.2 or 0.8 Tg N yr^{-1} estimated by Gu et al., (2015) and Wang et al., (2014), respectively), large-scale, spatially detailed N runoff trends and its attribution remain poorly understood.

Cropland N runoff, defined as a generation process of N loss via surface runoff, depends on environmental conditions and agricultural management practices (Zhang et al., 2016). This complexity makes large-scale N runoff difficult to estimate using empirical models. Plot-scale N runoff flux data from croplands are also difficult to scale up into spatially detailed maps because of spatio-temporally varying results (Shen et al., 2012). Currently, an export coefficient approach has been widely used to estimate cropland N runoff (Hao, 2006; Liu et al., 2010; Velthof et al., 2009; Wang et al., 2014). For example, the first National Pollution Census Program of China (NPCP) provided a collection of N runoff flux coefficients for different geographical regions in China, determined by fitting cross-sectional site data to an export-coefficient model (Wang et al., 2014). Nevertheless, substantial evidence gathered from field observations indicates that linear and homogeneous models are rarely capable of capturing the spatial variability of N runoff at regional scale (Schaefer and Alber, 2007; Sobota et al., 2009; Hou et al., 2016). This highlights the difficulty of accurately predicting its future evolution as well as quantifying the impacts on aquatic ecosystems.

While it is still challenging to attribute contributions of each individual driving factor (e.g., climate condition, agricultural management practices) to the cropland N runoff trend assessment, statistical correlation or regression analyses have been widely applied (Korsaeth and Eltun, 2000; Stalnacke et al., 2015) over past decades. However, this approach has two potential limitations. Firstly, statistical analyses of historical R_{TN} generally characterizes the related major drivers, thus includes the signals not only from the temporal trends, but also from inter-annual or decadal variability. Secondly, the use of statistical analysis generally assumes that the effects of drivers on N runoff are linear and independent of each other (Piao et al., 2015). However, a growing number of studies based on both data from field experiments and theoretical analyses indicated non-linear responses of N runoff to changes in driving factors as a consequence of complex interactions (Hou et al., 2016). Although these limitations in attribution analysis could be overcome through the application of process-based models (Hao, 2006; Abbaspour et al., 2015, Liu et al. 2016), core limitations of such simulation models are the large uncertainties arising from model structure and parameter choice (Schulz et al., 1999). One way to separate the contribution of natural and anthropogenic controls is to use the Kaya Identity concept developed in economics (Raupach et al., 2007), which is adopted when studying climate change and hydrological science (Streimikiene and Balezentis, 2016; Wang et al., 2015b).

To quantify and attribute cropland N runoff trends during past decades, we analyzed the data in this study is based on a upscaling model following a new simple attribution approach. Synthesized field measurements were used for model calibration and cross-validation based on the Bayesian Recursive Regression Tree algorithm version 2.0 (BRRT v2, Zhou et al., 2015), utilizing high-resolution gridded datasets including climate conditions, soil attributes, and agricultural management practices. First, we assessed inter-annual dynamics of cropland N runoff derived from the data-driven upscaling model to detect trends for the period from 1990 to 2012. Second, we compared the proportional change rate of each driver to upscaling results of R_{TN}, which allowed us to diagnose the contributions of different drivers. Finally, we discussed how each driver modulates the temporal trend of R_{TN} and the implications for site-specific N management.

2. Data and methodology

2.1 Dataset

Based on the National Pollution Census Program of China (NPCP) and datasets published by the scientific community, *in situ* measurements of N runoff and associated variables in each plot were collated from 100 experimental sites for both rice paddy and upland fields (i.e., as a flooded parcel of arable land used for growing rice and non-rice crops, respectively). Water samples were collected in the drainage outlet for each rainfall event in most of the measurements, where the runoff volume was consecutively measured within the observation period. N concentrations in water samples were analyzed using ultraviolet spectrophotometric methods, following the Standard Methods for the Examination of Water and Wastewater approach for China (SEPA, 2002). Precipitation within the observation period and soil properties (0-20 cm depth) at the beginning of the experiment were synchronously monitored. Missing values of soil properties or climatic factors at a few sites were supplemented with data from the China Soil Scientific Database (http://vdb3.soil.csdb.cn/) based on the corresponding soil type of the county or from the 0.1-degree China Meteorological Forcing Dataset (CMFD) v0106 (http://data.cma.cn/) depending on its geographic coordinates. Information on agricultural management practices including N fertilizer application rate, irrigation amount, fertilizer types, and crop types were recorded, including the timing of the application. The dataset comprised 535 site-years data (293 for upland

and 242 for rice paddy fields) (Fig. 1a and Supplementary Data S1), and can be considered representative of most major cropping areas except northwestern China (Fig. 1).

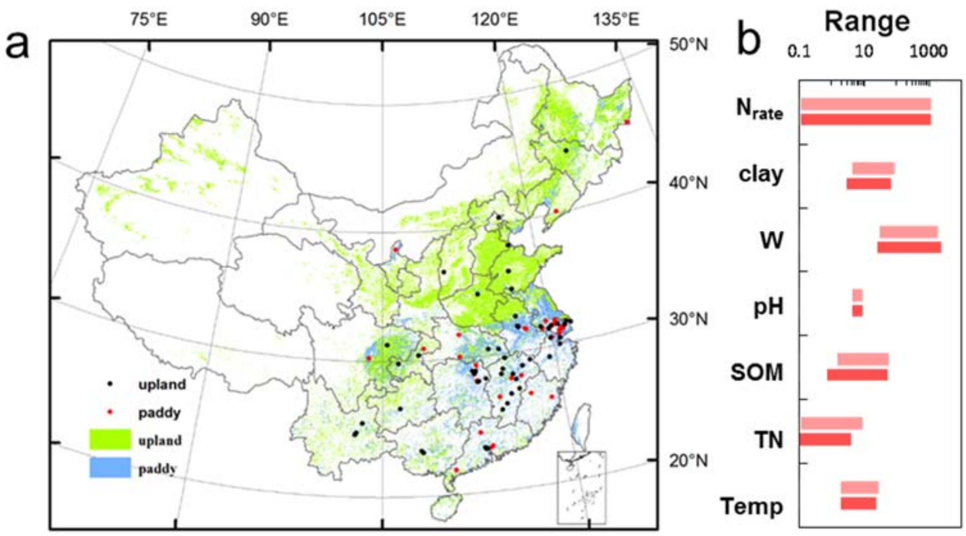

Figure 1. Location of experimental sites on cropland N runoff in China. Sixty-two experimental sites for upland are illustrated as black solid circles, whereas thirty-eight sites for paddy field are indicated as red solid circles. The ranges of each individual variable is illustrated as a light red bar for observational datasets and a dark red bar for croplands for the whole of China in panel b. The variables are N_{rate} (kg N ha^{-1}), clay content (Clay, %), water input (W, mm), soil pH, soil organic matter (SOM, g kg^{-1}), soil TN (g kg^{-1}) and air temperature (Temp, °C).

2.2 Data-driven upscaling model

We developed an upscaling model which accounts for the effects of environmental conditions and agricultural management (Eq. 1). Specifically, N fertilizer application rate (N_{rate}) and environmental conditions (x_k) are directly included as independent variables, whereas fertilizer application and crop types are considered as correction terms in the model:

$$R_{TNl} = RR_l(x_k)\cdot N_{rate} + R^0{}_l(x_k) + \varepsilon, \quad \forall l = 1,2,\ldots,L, \quad x_k \in \Omega_l \tag{1a}$$

where

$$RR_l = RR_l{}^*(x_k) \times CE_i(RR) \times CE_j(RR), \tag{1b}$$

$$R^0{}_l = R_l{}^{0,*}(x_k) \times CE_j(R^0), \tag{1c}$$

$$RR_l{}^*(x_k) = f(x_k)\cdot N_{rate} + g(x_k), \quad R_l{}^{0,*}(x_k) = h(x_k), \tag{1d}$$

and i and j represent the index of fertilizer types and crop types, respectively; l and L are the index and number of piecewise functions. x_k is climatic condition or soil attribute. Observations (Fig. S1) of air temperature, water input and soil clay content can be used as proxies to reflect the variations of soil temperature and water content within the observation period, respectively. RR^* and $R^{0,*}$ are the reference values when urea is applied and where wheat or rice are cultivated on experimental sites. Both are then adjusted to reflect different fertilizer and crop types to develop a specific RR and R^0 for a given scenario. The details of correction coefficients (*CE*s) can be found in Table S1. It should be noted that fertilizer types considered include urea, compound fertilizers, manure and/or crop residues, and ammonium bicarbonate. In addition, crop types distinguish between rice, wheat, maize, soybean, cotton, and other corps.

The Bayesian Recursive Regression Tree version 2 (Zhou et al., 2015), was subsequently used with observational data to determine optimal L, $f(x_k)$, $g(x_k)$, and $h(x_k)$. The detailed methodological approach of the BRRT v2 is described by Zhou et al. (2015)

and Text S2 in the Suppl. Mat.. The resulting calibrated model was applied to simulate spatial patterns of N runoff over Chinese croplands from 1990 to 2012 at a spatial resolution of 1 km. The details on input data used in this model, including N_{rate} by fertilizer and crop types, water input, clay content, air temperature, soil pH, soil organic matter (SOM), and soil N, are described in Table S2 and Fig. S2. Due to the lack of detailed information on the spatio-temporal changes in fertilization methods, timing, and cultivation practices in China, this information was not included in the data-driven upscaling model simulation presented here.

2.3 Structural decomposition analysis

We further applied a simplified attribution approach, 'Runoff Identity' (analogous to the Kaya Identity in economics), to assess the contribution of water input changes (*W*, the sum of precipitation and irrigation amounts), the fertilizer-to-water ratio (the ratio of fertilizer used to water input) and N runoff rate (i.e., the ratio of annual N runoff flux to fertilizer addition) to the relative rate of change of R_{TN} in China. The Runoff Identity combines the variables of regional averaged water inputs and fertilizer addition in a causal relationship to cropland N runoff (R_{TN}). R_{TN} is therefore regarded as the integration of the three variables:

$$R_{TN} = W\left(\frac{N_{rate}}{W}\right)\left(\frac{R_{TN}}{N_{rate}}\right) = w \cdot f \cdot e \tag{2}$$

We then defined the proportional change rate of a quantity $X(t)$ as $r(X)=X^{-1}\mathrm{d}X/\mathrm{d}t$ (with units [time]$^{-1}$). Because $((\mathrm{d}R_{TN}/\mathrm{d}t)/R_{TN}) = ((\mathrm{d}R_{TN}/\mathrm{d}t)/(wfe)) = ((\mathrm{d}w/\mathrm{d}t)/w) + ((\mathrm{d}f/\mathrm{d}t)/f) +$

($(de/dt)/e$) , the Runoff Identity for proportional change rate can be rewritten as

$$r(R_{TN}) = r(w) + r(f) + r(e) \qquad (3)$$

Using time-series data of *w*, *f* and *e*, we applied this approach to quantify the role of each driver in relation to changes of the R_{TN} trend. The theoretical proportional change rate, which was a sum of factors *w*, *f* and *e*, closely approximates the rate of R_{TN} that actually occurred. We calculate their rates of change over the whole period from 1990 to 2012 using a linear regression method, and normalized them by corresponding mean values, respectively. The relative contribution of each factor is the ratio of its proportional change rate to the proportional change rate of R_{TN} during the same period.

3. Results

3.1 Model performance

The data-driven upscaling model (Table S3) was evaluated by reviewing the coefficient of determination (R^2) and coefficient of variation (CV, calculated as the ratio of root-mean-squared error to mean value), which were 0.85 and 39% for rice paddy fields (n=242, Fig. 2a), and 0.85 and 50% for upland grain crops (n=293, Fig. 2b), respectively. The evaluation results suggest that most of the variance of R_{TN} could be explained by the model with acceptable bias. Model performance for R_{TN} per unit N fertilizer additions (RR) (R^2 = 0.71 and n=75 for rice paddy fields, Fig. 2c; R^2 = 0.40 and n = 146 for uplands, Fig. 2d) further indicate that our model is able to capture the sensitivity of R_{TN} to N inputs. Regionally, there are no evident differences in model performance of R_{TN} across the 7 regions (Fig. 2), but *RR* simulated by our model shows differences compared to observations in East China in particular. Additionally, a few simulated *RR* were different from the observations (Fig. 2), mainly due to the lack of spatially detailed data on specific fertilization methods, cultivation practices, or rainfall intensity in our models (Liu et al., 2016; Miyazato et al., 2010; Wang et al., 2015a; Xu et al., 2013).

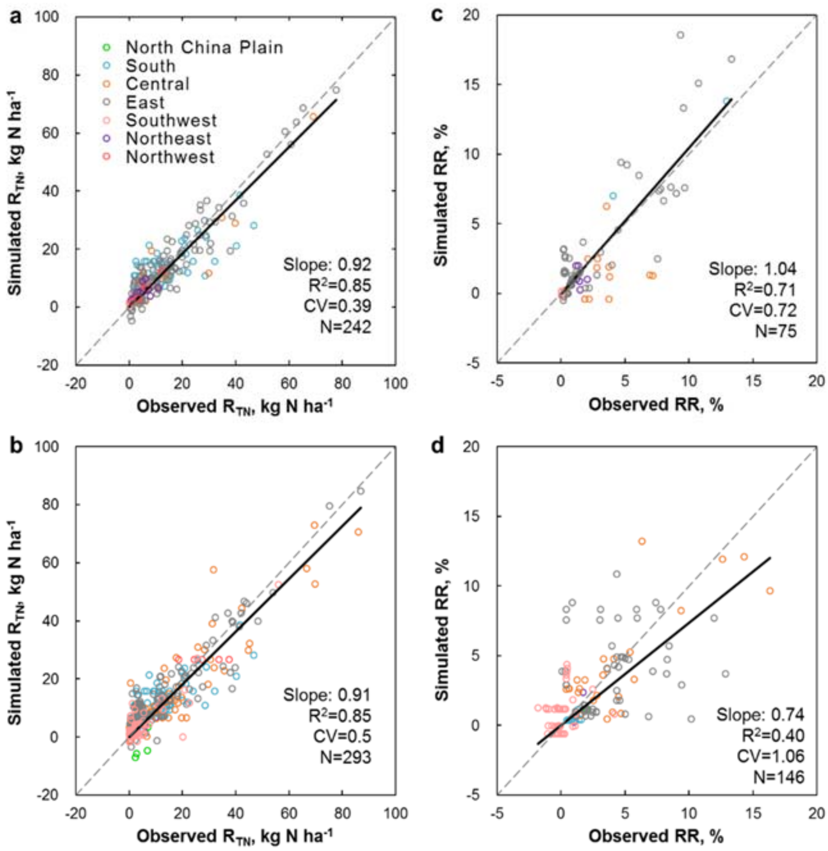

Figure 2. Calibration of R_{TN}, RR for paddy fields (panels a and c) and upland (panels b and d). The slope, R^2, and coefficient of variation (CV) are indicated in the insets at the bottom right of each panel. Dots are colored in Fig. 2 to indicate model performances in different regions in China.

3.2 N runoff trends and their spatial patterns

Figures 3a and 3b show the annual N runoff or runoff rate from China's rice paddy and upland soils from 1990 to 2012, respectively. In 1990, R_{TN} was 1.69 ± 0.80 Tg N yr^{-1} in China (σ is the standard deviation of N runoff due to the uncertainties of input data and model parameters), splitting into 0.46 ± 0.08 Tg N yr^{-1} for paddy field and 1.23 ± 0.51 Tg N yr^{-1} for upland (Fig. 3). More details of uncertainty estimation approach using Monte Carlo ensemble simulations can be found in Text S3. R_{TN} had increased by 2012 by 46 ± 11% for rice paddy fields and 31 ± 14% for uplands (σ is the standard deviation of N runoff changes occurring over a 23-year period; Fig. 3a and 3b).

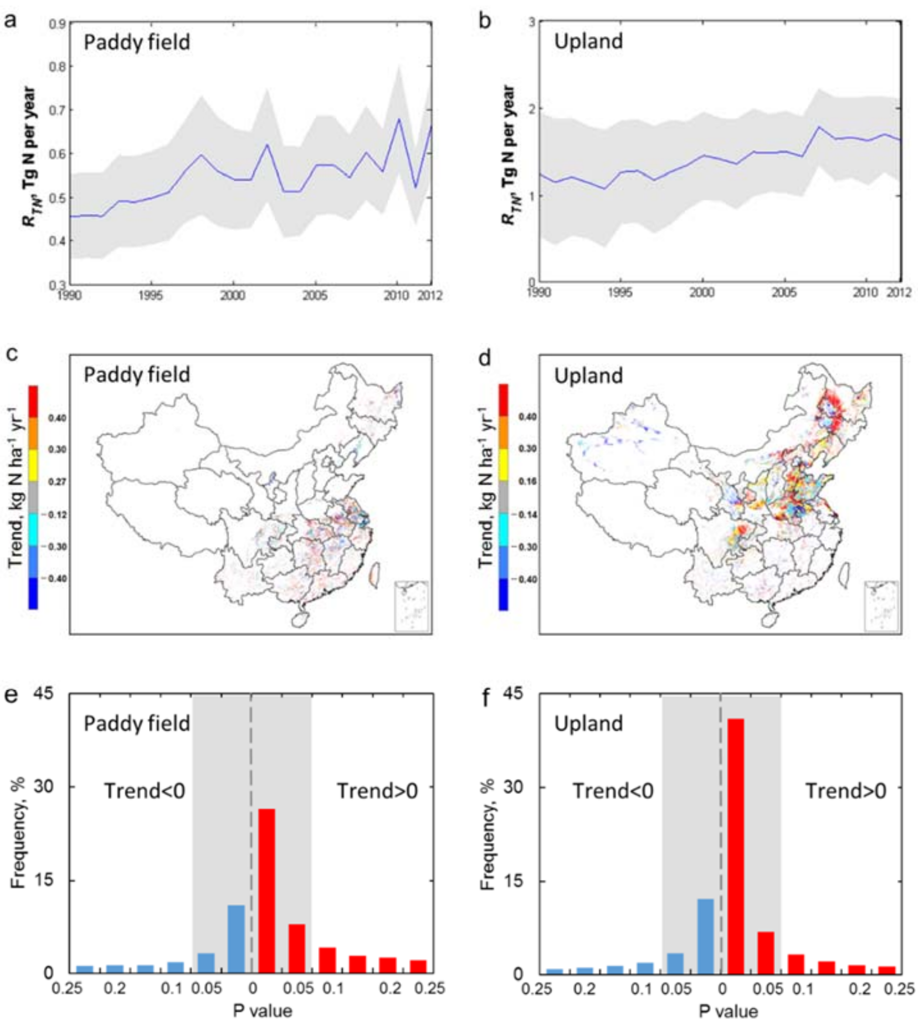

Figure 3. **Temporal trend of cropland N runoff during 1990-2012.** (a) paddy field; (b) upland; (c) spatial pattern of N runoff trend for paddy field; (d) the same as for c but for upland; (e) frequency distribution of the significance level (P-value) of N runoff trend for paddy field; (f) the same as for e but for upland. The P -value of N runoff trends for each pixel is estimated based on T test. The gray shaded areas in panels (a) and (b) reflect standard deviations based on uncertainty assessments (see Text S2).

Spatial patterns of the N runoff trends across China for the period from 1990 to 2012 were for the land area of China by applying the upscaling model are displayed in Figs. 3c and 3d. Both simulation results for rice paddy fields and uplands consistently showed that N runoff trend increased in most regions of China ($P < 0.01$ according to the Mann–Kendall test), while the magnitude of the R_{TN} trend varied for different croplands in China. For rice paddy soils, regions with the largest R_{TN} trend are generally found in southern China and parts of northeastern China (i.e., Amour-Ussuri-Songhua River Plain, defined in Fig. S3), where the trend of R_{TN} is generally larger than 0.4 kg N ha^{-1} yr^{-2}. However, regions that experienced a decreasing trend (14% of croplands) were located in the lower reaches of the Yangtze River Basin, Ningxia Plain, and part of the Sichuan Basin (Fig. S3), where the trend of R_{TN} is –0.12 kg N ha^{-1} yr^{-2}. For uplands, the highest values of the R_{TN} trend (>0.4 kg N ha^{-1} yr^{-2}) are found in northeast China, the Guanzhong Plain, and parts of the North China Plain and Sichuan Basin. In contrast, regions with a decreasing R_{TN} trend (16% of croplands) include the Shandong Peninsula, upper reaches of the Huaihe River Basin, and northwest China (–0.14 kg N ha^{-1} yr^{-2}). The R_{TN} trend is statistically insignificant (P>0.05) in less than 40% of croplands, mainly in the Yangtze River Basin, Shandong Peninsula and Shanxi province (Fig. 3e and 3f).

3.3 Attribution of N runoff trends at national scale

For rice paddy fields (Fig. 4a), the relative rate of change of R_{TN} at national scale was 1.2 % yr^{-1} over the last 23 years, which was primarily driven by a growing fertilizer-to-water ratio, but partly offset by the decline of water input (28%). For upland, the trend of R_{TN} also showed an increase (1.9% yr^{-1}; Fig. 4b) during the period 1990-2012, with the largest attributable contribution of fertilizer-to-water ratio and a positive proportional change rate of 2.4 % yr^{-1} which was partially offset by the decreased water input (–0.5 % yr^{-1}). Fig. 4 also illustrates the trend of each identity for rice paddy fields and uplands during different periods. The relative R_{TN} change rate for rice paddy field was 2.4 % yr^{-1} prior to the year 2000, but gradually reduced to 1.4 % yr^{-1} during the period of 1990-2005 and then less than 1.2 % yr^{-1} during 1990-2012, primarily due to the decreased growth rate of fertilizer-to-water ratio (3.0 to 1.5% yr^{-1}). However, the trend of R_{TN} for uplands increased from 0.15 % yr^{-1} before 2000 to 0.19 % yr^{-1} during the whole period. This could primarily be explained by the fact that the decrease of growing fertilizer-to-water ratio (from 2.9 to 2.4 % yr^{-1}) was totally offset by the change in the N runoff rate (from –0.9 to 0.01 % yr^{-1}).

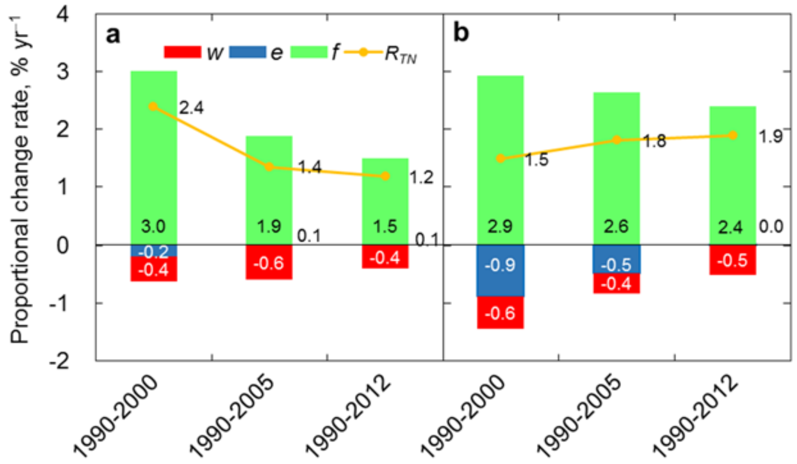

Figure 4. Proportional change rate of cropland N runoff and its drivers. (a) Paddy field; (b) upland. Contributions of the N runoff identity factors during the years 1990-2000, 1990-2005 and 1990-2012, including the water input of precipitation and irrigation (*w*), N runoff rate (*e*) and fertilizer-to-water ratio (*f*).

3.4 Spatial patterns of N runoff trend attributed to different drivers

As demonstrated in Fig. 5, the contributions from three main driving factors to the trend of R_{TN} were highly spatially heterogeneous across different provinces. For rice paddy fields, fertilizer-to-water ratio was the dominant factor for R_{TN} trends in most regions in China, whereas N runoff rate and water input could be attributed to drive the trends in N runoff in eastern coastal regions, and Weihe River Basin (inset plot of Fig. 5a). More specifically, fertilizer-to-water ratio factor alone increased N runoff at a rate of 1.14 ± 1.05 % yr^{-1} in most rice-cropping areas in southeastern China (Fig. 5a) while N runoff rate had a positive effect on the R_{TN} trend in most regions in southern China at an average of change rate of 1.32 ± 0.98% yr^{-1}. However, N runoff rate had a more substantial negative effect on the R_{TN} trend in the other regions and the average trend of R_{TN} attributed to N runoff rate is -1.12 ± 1.07 % yr^{-1}. In contrast to those two driving factors, the relative contribution of water input to the R_{TN} trend was minor, but remained consistently negative for rice paddy fields across the whole country (<–0.14 % yr^{-1}), except for Taiwan (1.06 % yr^{-1}), Shaanxi (0.99 % yr^{-1}), and Ningxia provinces (0.31 % yr^{-1}).

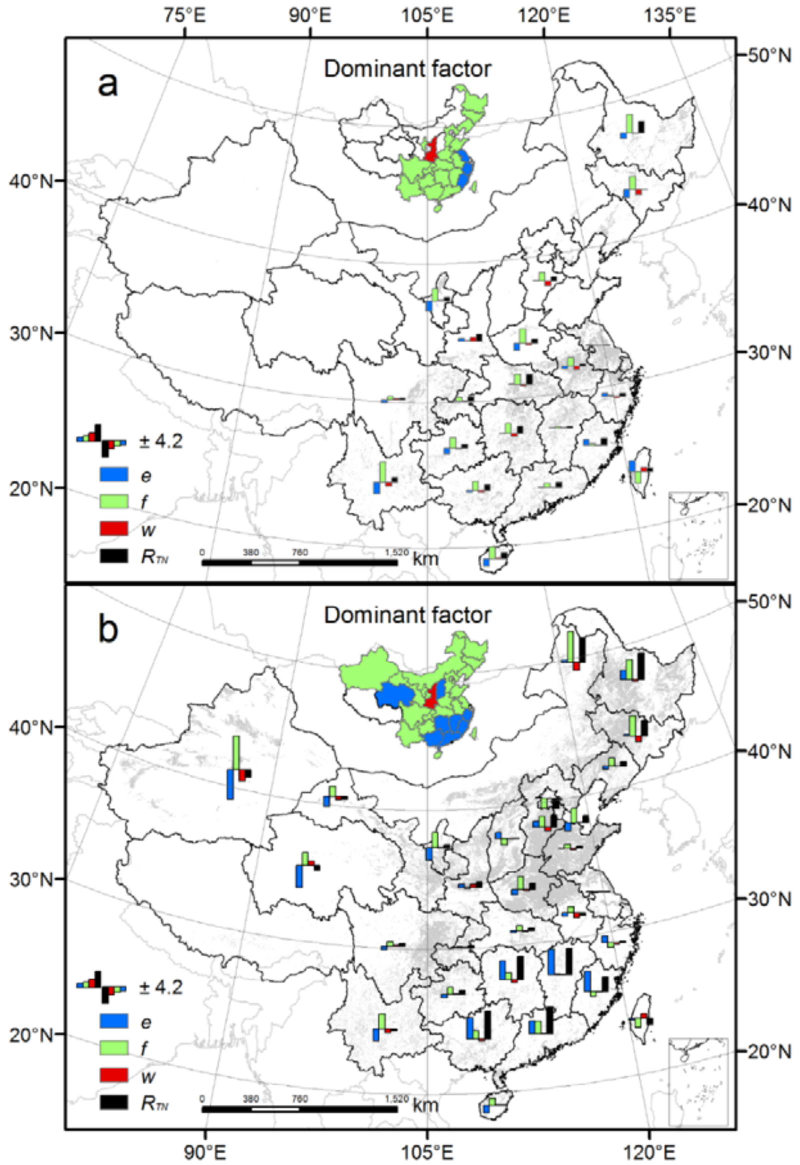

Figure 5. Trends in N runoff and its drivers during the period 1990-2012 at provincial scale. (a) Paddy fields; (b) upland. The dominant driving factors for the R_{TN}

trend in each province are shown in the insets above the maps. The grey area shows the spatial pattern of upland or paddy fields in China.

Fertilizer-to-water ratio contributed more to the R_{TN} trend for uplands than for rice paddy fields in the North China Plain and northeast Plain only. A positive effect of fertilizer-to-water ratio on the R_{TN} trend was largely offset by N runoff rate changes across southern China and western China, where the trends of R_{TN} attributed to N runoff rate averaged at 4.36 ± 1.67 % yr^{-1} and -3.08 ± 2.40 % yr^{-1}, respectively. On the other hand, the model estimates indicate that N runoff rate changes may result in R_{TN} increases in southern China (except for Hainan and Taiwan), which were one-fold higher than the negative effect found across most of northern China. Although there was no apparent difference in spatial patterns as to water input trends between upland and paddy field (Fig. 5), the relative contribution of water input to the R_{TN} trend for upland was less than that for paddy field. In contrast to other regions, water input in Shaanxi, Taiwan and Hainan provinces has significantly increase ($P < 0.01$). The increase in trend of R_{TN} due to water input change in Shanxi was larger than due to N runoff rate and fertilizer-to-water ratio for both crop types. The observations in Taiwan and Qinghai show that water input change played an important role in R_{TN} increase, albeit less than the other two driving factors, accounting for 1.2 % yr^{-1} and 1.1 % yr^{-1} of the trend of R_{TN}. In summary, the effects of agricultural management practices, including fertilization and irrigation schemes, outweigh the influence of current climate change on model-derived R_{TN} trend increase for both paddy field and upland.

4. Discussion

Our findings generally agree well with most prior works, with a few exceptions. For example, Gu et al. (2015) applied an integrated N budget model to constrain the magnitude and trend of N runoff from China's croplands, with an estimate of R_{TN} of 2.1±0.2 Tg yr^{-1} with a relative change rate of 1.8 % yr^{-1} during the period 1990-2010. In our study, we explicitly incorporated the non-linear and spatially varied responses of an R_{TN} model at multiple N input levels and reached very similar estimates of total N runoff (1.7±0.2 Tg yr^{-1}) and trend (1.7 % yr^{-1}) while explicitly accounting for spatial variability during the same period (Fig. S4). In addition, Ti and Yan (2013) indicated that the fertilizer-induced N runoff in the Huanghe River Basin, the Yangtze River Basin, and the Paerl River Basin was 1.06 Tg yr^{-1} in 2010 with a relative change rate of 1.4 % yr^{-1} during the period from 1990-2010, which is also comparable to our results (0.72 Tg yr^{-1} in 2010 and 1.7 % yr^{-1}). In general, using a new data-driven upscaling model, our estimates derived from a large network of cropland N runoff observations, provide novel insights into the spatially detailed N runoff trend for China's croplands.

By developing a novel structured decomposition approach for a 'Runoff Identity' (see section 2.3), we are able to accurately identify and quantify the contribution from each individual driver including climatic and human-induced variables to R_{TN} trend. Our results suggest that fertilization (or fertilizer-to-water ratio) is the dominant driver of R_{TN} trends for both rice paddy fields and uplands across most of the country, which is consistent with experimental results at multiple N input levels (Liang et al., 2005; Shi et al., 2010; Yu, 2011). Indeed, over the last two decades, China experienced a growth rate in N fertilizer application of more than 4.0 kg N ha^{-1} yr^{-1} on average in response to a continuous increase in crop production (Fig. S5a). Previous studies suggest that this high rate of N additions to agricultural systems resulted in an increase in soil residual N (Yan et al., 2014). Such accumulated residual N was eventually transferred into aquatic ecosystems (Rasouli et al., 2014). Conversely, eastern and southern coastal regions in Mainland China remained largely unchanged with regard to N application rates and even rates even decreased in Taiwan (Fig. S5a). The N runoff rate in these regions therefore becomes the primary driving force for R_{TN} trends.

Likewise, we quantified the contribution of water input to the R_{TN} trend increase in China. For rice paddy fields, our model suggests that the decreasing water input offsets 27% of the impact of fertilization on the increasing R_{TN} trend at the national scale, and this offset effect is more clearly observed in northern China than in south (Fig. 5). Previous studies indicated that R_{TN} tends to increase with water input (Gao et al., 2016; Hou et al., 2016), because high precipitation and irrigation events in turn resulted in large runoff pulses (Sorooshian et al., 2014). As we illustrated, the decline in water input mainly occurred due to the decrease in irrigation inputs, rather than a marked change in precipitation patterns, except in Taiwan, Hainan and parts of northwestern China (Fig. S6a). Improving the irrigation efficiency could be an effective measure to reduce the overall amount of water used for irrigation in most provinces, whereas the expansion of irrigated area dominates the growth of irrigation mainly in the Northeast Plain, Sichuan Basin, and Yunnan-Guizhou Plateau. Similar drivers and patterns of irrigation trends are found for upland all over the country (Fig. S6b). It should be noted that our per-area irrigation dataset was compiled based on total values at municipal level, rather than on crop-specific amounts (Fig. S5b). Therefore, it would be valuable if future research focused on surveys to address this issue by gathering data per-area irrigation among different crops in each municipal area.

Our results attributing the contribution by different factors also indicate that the N runoff rate positively affected the R_{TN} trend for uplands across most of southern China, but in general had a negative effect for rice paddy fields (Fig. 5). To interpret such distinct effects on N runoff rates, we conducted two types of scenario assessments to separate the impact of changes in environmental conditions or agricultural management practices: a control simulation with all conditions and practices varying from 1990 to 2012 and an experimental simulation with one condition or practice fixed at year 1990 levels. The difference was considered as the response to one change in conditions or practices. SOM was identified as the dominant factor for the trends of N runoff rate for both uplands and rice paddy fields nationwide, followed by N_{rate} and water input (Fig.

S7). Increased SOM led to N runoff rate growth for uplands, but a decline for rice paddy fields at provincial level during the period1990-2012 (Fig. S8). This result was also confirmed by observations from 63 field sites across China (Fig. S9), and could be explained by the difference in the generation process of N runoff. Upland N runoff begins when raindrops hit the ground and detach soil particles by splash. The sediments eroded from upland fields carry adsorbed N that is subsequently transported downstream. Therefore, high SOM may increase the risk of upland N runoff during rainfall events (Liu et al., 2014). In contrast, N runoff from paddy fields increases when rainfall input exceeds its storage capacity. Overflow through the paddy field levee carries dissolved N into ponding water and rainfall-driven interstitial runoff of nitrate at the soil-water interface to the surrounding water bodies (Huang et al., 2014; Higashino and Stefan, 2014). High SOM improves the adsorption of soil N in ponding water thus lowers the magnitude of N runoff from paddy fields. Additionally, high SOM benefits upland N mineralization under aerobic environment, resulting in increases in soil inorganic N availability and hence N runoff. Little inorganic N, however, will be released from SOM in paddy field under anaerobic environment, which helps reducing N runoff (Wu et al., 2017).

In this study, we comprehensively quantified and analyzed the attribution factors for N runoff trends in China's croplands. However, we found that some results for simulated N runoff were significantly different from observations (Fig. 2). Previous experiments showed that N runoff or N runoff rate were also changed following different fertilization (e.g., methods, timing), irrigation schemes, or rainfall intensity (Liu et al., 2016; Miyazato et al., 2010; Wang et al., 2015a; Xu et al., 2013). For example, field trials highlighted that the application of controlled release N fertilizers significantly reduced N runoff by 48-72% compared to top-dressing fertilization for paddy fields. Similarly, the application of optimized irrigation methods significantly reduced N runoff by 24% compared to flooding irrigation (Yang et al., 2015); N runoff from paddy fields was not only passively generated by monsoon rain in China, but also a consequence of human-induced drainage before transplanting (Yan et al., 2016). However, the current upscaling model did not fully consider such management practices. Meanwhile, air temperature and clay content were used in this study as proxies for soil temperature and soil water content within the experimental period, respectively, due to the lack of long-term observations across China. Although previous works have found a significant linear relationship between air and soil temperatures or between clay and water contents (Zheng et al., 1993; Wäldchen et al., 2012), more robust estimations of soil temperature and water content become another question to be undertaken by future studies. In addition, *in situ* measurements of N runoff are scarce in Northwest China (e.g., Xinjiang province), leading to large uncertainty in R_{TN} estimates in this regions. Previous studies indicated that the dominant pathways of N losses would be ammonia volatilization to the atmosphere and N leaching to aquifers (Gao et al., 2016; Van Damme et al., 2017), rather than surface N runoff. More importantly, this region accounts for only 8.6% of

N fertilizer application and 11% of the sowing area in China and has a low N runoff rate observed in the NPCP (0. 34 ± 0.26 %). Therefore, N runoff in Northwest China makes a small overall contribution to the total N runoff of Chinese croplands. To confirm the contribution from Northwest China, more observations should be conducted in the future to verify R_{TN} estimates. Furthermore, data from field manipulation experiments on the response of R_{TN} to environmental conditions (e.g., SOM) is lacking and would be useful to constrain our upscaling model. Therefore, further efforts to make widespread measurements and to carry out field manipulation experiments for R_{TN} are necessary to improve the reliability of such model simulations.

In summary, cropland N runoff has been increasing significantly in China for the period 1990-2012. At a national scale, increases in fertilizer application and decreases in irrigation amounts were identified as the most likely causes for the N runoff trend. The positive contribution of N runoff rate to the R_{TN} trend is more evident in southern China than in the north. We expect a continuously decreasing trend in irrigation amounts into the future, and fertilizer application rates likely to plateau, since China aims to improve water use as well as fertilizer N application efficiencies through the action plans like clean water and “zero-increase fertilizer use” (Ju et al., 2016). However, current projections on climate change suggest that precipitation, particularly extreme rainfall events, will increase. This might further lead to N runoff and N runoff rate increase in the future. In addition to the expected improvements on N use efficiency and water use efficiency in China’s croplands, applying effective management approaches that generate benefits for both N runoff and crop yields are urgently required to design more efficient and sustainable agricultural N management. Improving the representations associated with the effects of agricultural management practices and understanding the response of N runoff to environmental conditions should be the priorities for the agricultural modeling.

Acknowledgements

This study was supported by the National Key Research and Development Program of China (2016YFD0800501), the National Natural Science Foundation of China (41671464, 41530528, and 41561134016), National Science Foundation of Zhejiang Province (LR15G030001), and 111 Project (B14001). We appreciated HWSD and CMFD teams for providing soil and climate datasets, and authors who measured, analyzed, and published data of N runoff used here.

Appendix A. Supplementary data

Supplementary information related to this article can be found online, including Supplementary Data S1, Text S1 to S3, Tables S1 to S4, and Figures S1 to S9.

References

Abbaspour, K.C., Rouholahnejad, E., Vaghefi, S., Srinivasan, R., Yang, H., Klove, B., 2015. A continental-scale hydrology and water quality model for Europe:

Calibration and uncertainty of a high-resolution large-scale SWAT model. Journal of Hydrology 524, 733-752.

Chen, X., Cui, Z., Fan, M., Vitousek, P., Zhao, M., Ma, W., Wang, Z., Zhang, W., Yan, X., Yang, J., Deng, X., Gao, Q., Zhang, Q., Guo, S., Ren, J., Li, S., Ye, Y., Wang, Z., Huang, J., Tang, Q., Sun, Y., Peng, X., Zhang, J., He, M., Zhu, Y., Xue, J., Wang, G., Wu, L., An, N., Wu, L., Ma, L., Zhang, W., Zhang, F., 2014. Producing more grain with lower environmental costs. Nature 514, 486-489.

Cherry, K.A., Shepherd, M., Withers, P.J., Mooney, S.J., 2008. Assessing the effectiveness of actions to mitigate nutrient loss from agriculture: a review of methods. Science of the Total Environment 406, 1-23.

Cui, Z., Wang, G., Yue, S., Wu, L., Zhang, W., Zhang, F., Chen, X., 2014. Closing the N-Use efficiency gap to achieve food and environmental security. Environmental Science & Technology 48, 5780-5787.

Gao, S., Xu, P., Zhou, F., Yang, H., Zheng, C., Cao, W., Tao, S., Piao, S., Zhao, Y., Ji, X., Shang, Z., Chen, M., 2016. Quantifying nitrogen leaching response to fertilizer additions in China's cropland. Environmental Pollution 211, 241-251.

Gu, B., Ju, X., Chang, J., Ge, Y., Vitousek, P.M., 2015. Integrated reactive nitrogen budgets and future trends in China. Proceedings of the National Academy of Sciences 112, 8792-8797.

Hao, F.H., Yang, S.T., Cheng, H.G., Bu, Q.Y., Zheng, L.F., 2006. A method for estimation of non - point source pollution load in the large - scale basins of China (in Chinese). Acta Scientiae Circumstantiae 26, 375 - 383

Harrison, J.A., Seitzinger, S.P., Bouwman, A.F., Caraco, N.F., Beusen, A.H.W., Vorosmarty, C.J., 2005. Dissolved inorganic phosphorus export to the coastal zone: Results from a spatially explicit, global model. Global Biogeochemical Cycles 19, 367-384.

Higashino, M., Stefan, H.G., 2014. Modeling the effect of rainfall intensity on soil-water nutrient exchange in flooded rice paddies and implications for nitrate fertilizer runoff to the Oita River in Japan. Water Resources Research 50, 8611-8624.

Hou, X.K., Zhou, F., Leip, A., Fu, B.J., Yang, H., Chen, Y., Gao, S.S., Shang, Z.Y., Ma, L.K., 2016. Spatial patterns of nitrogen runoff from Chinese paddy fields. Agriculture, Ecosystems & Environment 231, 246-254.

Huang, H., Ouyang, W., Guo, B., Shi, Y., Hao, F., 2014. Vertical and horizontal distribution of soil parameters in intensive agricultural zone and effect on diffuse nitrogen pollution. Soil & Tillage Research 144, 32-40.

Ju, X.T., Gu, B.J., Wu, Y.Y., Galloway, J.N., 2016. Reducing China's fertilizer use by increasing farm size. Global Environmental Change 41, 26-32.

Liu, W.F., Yang, H., Liu, J.G., Azevedo, L.B., Wang, X.Y., Xu, Z.X., Abbaspour, K.C., Schulin, R., 2016. Global assessment of nitrogen losses and trade-offs with yields from major crop cultivations. Science of the Total Environment 572, 526-537.

Raupach, M. R., Marland, G., Ciais, P., Le Quéré, C., Canadell, J. G., Klepper, G., Field,

C. B., 2007. Global and regional drivers of accelerating CO_2 emissions. Proceedings of the National Academy of Sciences 104, 10288-10293.

Korsaeth, A., Eltun, R., 2000. Nitrogen mass balances in conventional, integrated and ecological cropping systems and the relationship between balance calculations and nitrogen runoff in an 8-year field experiment in Norway. Agriculture, Ecosystems & Environment 79, 199-214.

Leip, A., Britz, W., Weiss, F., de Vries, W., 2011. Farm, land, and soil nitrogen budgets for agriculture in Europe calculated with CAPRI. Environmental Pollution 159, 3243-3253.

Liang, X.Q., Tian, G.M., Li, H., Chen, Y.X., Zhu, S., 2005. Study on characteristic of nitrogen and phosphorus loss from rice field by natural rainfall runoff. Journal of Soil Water Conservation 19, 59-63.

Liu, J.G., You, L.Z., Amini, M., Obersteiner, M., Herrero, M., Zehnder, A.J.B., Yang, H., 2010. A high-resolution assessment on global nitrogen flows in cropland. Proceedings of the National Academy of Sciences 107, 8035-8040.

Liu, Q., Li, Z.B., Li, P., 2014. Effect of runoff dynamic on sediment and nitrogen losses in an agricultural watershed of the southern Shaanxi region, China. Clean-Soil Air Water 42, 56-63.

Miyazato, T., Mohammed, R.A., Lazaro, R.C., 2010. Irrigation management transfer (IMT) and system of rice intensification (SRI) practice in the Philippines. Paddy and Water Environment 8, 91-97.

Mueller, N. D., Gerber, J. S., Johnston, M., Ray, D. K., Ramankutty, N., & Foley, J. A. 2012. Closing yield gaps through nutrient and water management. Nature, 490, 254-257.

Paerl, H.W., Hall, N.S., Peierls, B.L., Rossignol, K.L., 2014. Evolving paradigms and challenges in estuarine and coastal eutrophication dynamics in a culturally and climatically stressed world. Estuaries and Coasts 37, 243-258.

Piao, S., Yin, G., Tan, J., Cheng, L., Huang, M., Li, Y., Liu, R., Mao, J., Myneni, R.B., Peng, S., Poulter, B., Shi, X., Xiao, Z., Zeng, N., Zeng, Z., Wang, Y., 2015. Detection and attribution of vegetation greening trend in China over the last 30 years. Global Change Biology 21, 1601-1609.

Rasouli, S., Whalen, J.K., Madramootoo, C.A., 2014. Review: reducing residual soil nitrogen losses from agroecosystems for surface water protection in Quebec and Ontario, Canada: best management practices, policies and perspectives. Canadian Journal of Soil Science 94, 109-127.

Raymond, P.A., David, M.B., Saiers, J.E., 2012. The impact of fertilization and hydrology on nitrate fluxes from Mississippi watersheds. Current Opinion in Environmental Sustainability 4, 212-218.

Seitzinger, S.P., Mayorga, E., Bouwman, A.F., Kroeze, C., Beusen, A.H.W., Billen, G., Van Drecht, G., Dumont, E., Fekete, B.M., Garnier, J., Harrison, J.A., 2010. Global river nutrient export: A scenario analysis of past and future trends. Global Biogeochemical Cycles 24, 2621-2628.

Schaefer, S.C., Alber, M., 2007. Temperature controls a latitudinal gradient in the proportion of watershed nitrogen exported to coastal ecosystems. Biogeochemistry 85, 333-346.

SEPA, 2002. Standard methods for the examination of water and wastewater version 4. Beijing: China Environmental Science Press.

Shen, Z.Y., Liao, Q., Hong, Q., Gong, Y.W., 2012. An overview of research on agricultural non-point source pollution modelling in China. Separation and Purification Technology 84, 104-111.

Shi, L.H., Ji, X.H., Li, H.S., Tian, F.X., Peng, H., Liu, S.B., 2010. Nitrogen and phosphorus losses from surface runoff under different application in the double cropping rice fields in Hunan (in Chinese). Chinese Journal of Agrometeorology 31, 551-557.

Sobota, D.J., Harrison, J.A., Dahlgren, R.A., 2009. Influences of climate, hydrology, and land use on input and export of nitrogen in California watersheds. Biogeochemistry 94, 43-62.

Sorooshian, S., AghaKouchak, A., Li, J.L., 2014. Influence of irrigation on land hydrological processes over California. Journal of Geophysical Research-Atmospheres 119, 13137-13152.

Stalnacke, P., Pengerud, A., Vassiljev, A., Smedberg, E., Morth, C.M., Hagg, H.E., Humborg, C., Andersen, H.E., 2015. Nitrogen surface water retention in the Baltic Sea drainage basin. Hydrology and Earth System Sciences 19, 981-996.

Streimikiene, D., Balezentis, T., 2016. Kaya identity for analysis of the main drivers of GHG emissions and feasibility to implement EU "20-20-20" targets in the Baltic States. Renewable & Sustainable Energy Reviews 58, 1108-1113.

Ti, C.P., Yan, X.Y., 2013. Spatial and temporal variations of river nitrogen exports from major basins in China. Environmental Science and Pollution Research 20, 6509-6520.

Tilman, D., Balzer, C., Hill, J., Befort, B.L., 2011. Global food demand and the sustainable intensification of agriculture. Proceedings of the National Academy of Sciences, USA 108, 20260-20264.

Van Damme, M.; Whitburn, S.; Clarisse, L.; Clerbaux, C.; Hurtmans, D.; Coheur, P. F. Version 2 of the IASI NH3 neural network retrieval algorithm; near-real time and reanalysed datasets. Atmos. Meas. Technol. Disc. 2017,, doi:110.5194/amt-2017-239

Velthof, G.L., Oudendag, D., Witzke, H.P., Asman, W.A., Klimont, Z., Oenema, O., 2009. Integrated assessment of nitrogen losses from agriculture in EU-27 using MITERRA-EUROPE. Journal of Environmental Quality 38, 402-417.

Wäldchen, J., Schoning, I., Mund, M., Schrumpf, M., Bock, S., Herold, N., Totsche, K.U., Schulze, E.D., 2012. Estimation of clay content from easily measurable water content of air-dried soil. Journal of Plant Nutrition and Soil Science 175, 367-376.

Wang, J., Lu, G.A., Guo, X.S., Wang, Y.Q., Ding, S.W., Wang, D.Z., 2015a. Conservation tillage and optimized fertilization reduce winter runoff losses of nitrogen and phosphorus from farmland in the Chaohu Lake region, China. Nutrient Cycling in Agroecosystems 101, 93-106.

Wang, S., Fu, B., Piao, S., Lü, Y., Ciais, P., Feng, X., Wang, Y., 2015b. Reduced sediment transport in the Yellow River due to anthropogenic changes. Nature Geoscience 9, 38-41.

Wang, X.L., Feng, A.P., Wang, Q., Wu, C.Q., Liu, Z., Ma, Z.S., Wei, X.F., 2014. Spatial variability of the nutrient balance and related NPSP risk analysis for agro-ecosystems in China in 2010. Agriculture, Ecosystems & Environment 193, 42-52.

Wu, L., Tang, S.R., He, D.D., Wu, X., Shaaban, M., Wang, M.L., Zhao, J.S., Khan, I., Zheng, X.H., Hu, R.G., Horwath, W.R., 2017. Conversion from rice to vegetable production increases N_2O emission via increased soil organic matter mineralization. Science of the Total Environment 583, 190-201.

Xu, J., Shan, L.N., Yu, D.P., Li, Z.L., He, Y.F., 2013. Effects of different fertilization modes on nitrogen use efficiency of cabbages and nitrogen loss from vegetable field (in Chinese). Journal of Zhejiang University 39, 556-564.

Yan, R., Gao, J., Huang, J., 2016. WALRUS-paddy model for simulating the hydrological processes of lowland polders with paddy fields and pumping stations. Agricultural Water Management 169, 148-161.

Yan, X., Ti, C., Vitousek, P., Chen, D., Leip, A., Cai, Z., Zhu, Z., 2014. Fertilizer nitrogen recovery efficiencies in crop production systems of China with and without consideration of the residual effect of nitrogen. Environmental Research

Letters 9, 095002.

Yang, S.H., Peng, S.Z., Xu, J.Z., He, Y.P., Wang, Y.J., 2015. Effects of water saving irrigation and controlled release nitrogen fertilizer managements on nitrogen losses from paddy fields. Paddy and Water Environment 13, 71-80.

Yu, Q.G., Ye, J., Ma, J.W., Sun, W.C., Wang, Q., Jiang, L.N., Fu, J.R., Chen, Y., 2011. Effects of different nitrogen applied levels on nitrogen runoff loss in oilseed rape fields (in Chinese). Journal of Soil and Water Conservation 25, 22-25.

Zhang, X., Davidson, E.A., Mauzerall, D.L., Searchinger, T.D., Dumas, P., Shen, Y., 2015. Managing nitrogen for sustainable development. Nature 528, 51-59.

Zhang, Y., Zhou, Y., Shao, Q., Liu, H., Lei, Q., Zhai, X., Wang, X., 2016. Diffuse nutrient losses and the impact factors determining their regional differences in four catchments from North to South China. Journal of Hydrology 543, 577-594.

Zheng, D., Hunt Jr., E.R. and Running, S.W. 1993. A daily soil temperature model based on air temperature and precipitation for continental applications. Climate Research, 2, 183-191..

Zhou, F., Shang, Z., Zeng, Z., Piao, S., Ciais, P., Raymond, P.A., Wang, X., Wang, R., Chen, M., Yang, C., Tao, S., Zhao, Y., Meng, Q., Gao, S., Mao, Q., 2015. New model for capturing the variations of fertilizer-induced emission factors of N_2O. Global Biogeochemical Cycles 29, 885-897.